Fe or Co occupies the inversion centers with calcium in mirror plane positions, isostructural with monticellite ($CaMgSiO_4$). Attempts to synthesize $CaNiSiO_4$ proved unsuccessful. In $CaMnSiO_4$, the manganese moments align in antiferromagnetic chains along **b** with spin directions collinear with **c**. The cobalt salt has a large magnetic cell similar to Ni_2SiO_4, but systematic absences suggest a ferromagnetic direct interaction. $CaFeSiO_4$ remains paramagnetic to low temperatures.

Only superexchange interactions occur in the lithiophilite–triphylite group where the transition-metal ions are partially replaced by the smaller Li^+ ion. As mentioned previously, the $LiMPO_4$ (M = Mn, Fe, Co, Ni) compounds possess similar magnetic structures. M–O–M superexchange interactions give rise to antiferromagnetic puckered-planes orthogonal to **a**. There are no direct or superexchange linkages between these planes, and it is necessary to postulate long-range interactions, such as the Mn–O–P–O–Mn triple exchange suggested by Mays (1963).

In $LiMnPO_4$ and Mn_2SiO_4 the spins align along **a**, the direction minimizing the magnetic dipole energy. **b** is the preferred direction for the iron and cobalt compounds, in which spin-orbit and crystal field interactions are often decisive. The spin direction of the magnetically ordered lithiophilite–triphylite series must depend on composition since the magnetic structures of the end members differ. Susceptibility measurements on $LiMn_{0.7}Fe_{0.3}PO_4$ single crystals (Bozorth & Kramer, 1959) specify **b** as the spin direction, like $LiFePO_4$. The change in spin direction therefore takes place in manganese-rich compositions near $LiMnPO_4$.

References

BERTAUT, E. F. (1963). *Magnetism,* Vol. III, 157. (G. T. Rado & H. Suhl, Editors). New York & London: Academic Press.

BOZORTH, R. M. & KRAMER, V. (1959). *J. Phys. Radium,* **20**, 393.

CARON, L. G., SANTORO, R. P. & NEWNHAM, R. E. (1965). *J. Phys. Chem. Solids,* **26**, 927.

COX, D. E., FRAZER, B. C., ALMODOVAR, I. & KAY, M. I. (1965). Abstracts A.C.A. Annual Meeting, Gatlinburg, Tenn. p. 47.

DESTENAY, D. (1950). *Mém. Soc. Roy. Sci. Liège,* **10**, 5.

FONER, S. (1959). *Rev. Sci. Instrum.* **30**, 548.

GELLER, S. & DURAND, J. L. (1960). *Acta Cryst.* **13**, 325.

GOODGAME, M. & COTTON, F. A. (1961). *J. Chem. Phys.* **65**, 791.

KELLEY, K. K. (1941). *J. Amer. Chem. Soc.* **63**, 2750.

KONDO, H. & MIYAHARA, S. (1963). *J. Phys. Soc., Japan,* **18**, 305.

MAYS, J. M. (1963). *Phys. Rev.* **131**, 38.

NEWNHAM, R. E., CARON, L. G. & SANTORO, R. P. (1966). *J. Amer. Ceram. Soc.* In the press.

NEWNHAM, R. E. & REDMAN, M. J. (1965). *J. Amer. Ceram. Soc.* **48**, 547.

NEWNHAM, R., SANTORO, R., FANG, J. & NOMURA, S. (1965). *Acta Cryst.* **19**, 147.

NOMURA, S., SANTORO, R., FANG, J. & NEWNHAM, R. (1964). *J. Phys. Chem. Solids,* **25**, 901.

SANTORO, R. P. & NEWNHAM, R. E. (1964). *J. Amer. Ceram. Soc.* **47**, 491.

SANTORO, R. P., NEWNHAM, R. E. & NOMURA, S. (1966). *J. Phys. Chem. Solids.* **27**, 655.

SANTORO, R. P., SEGAL, D. J. & NEWNHAM, R. E. (1966). *J. Phys. Chem. Solids.* **27**, 1192.

ZAMBONINI, F. & MALOSSI, L. (1931). *Z. Kristallogr.* **80**, 442.

Acta Cryst. (1967). **22**, 347

Five New Zinc Sulphide Polytypes: 10*L* (8 2); 14*L* (5 4 2 3); 24*L* (5 3)$_3$; 26*L* (17 4 2 3) and 28*L* (9 5 5 9)

BY O. BRAFMAN, E. ALEXANDER AND I. T. STEINBERGER

Department of Physics, The Hebrew University, Jerusalem, Israel

(*Received* 13 *May* 1966)

The layer sequences of some ZnS polytypes have been determined by comparing observed X-ray reflexion intensities with those calculated by a computer. It is demonstrated that birefringence measurements facilitate these determinations, since the number of elements of the Zhdanov symbol can be known from measuring the degree of the birefringence. Differences of polytypism in SiC and ZnS are discussed briefly.

Introduction

It has been known (Frondel & Palache, 1950), that both natural and artificially grown ZnS crystals often exhibit polytypism. Still, very little is known about polytypism in ZnS, since even in the cases where the existence of a polytype has been reported, usually only the periodicity of the structure is given and the actual stacking sequence is missing. The only exceptions are 6*L* [six-layer periodicity, (3 3)], 15*L* (3 2)$_3$ (Frondel & Palache, 1950), 8*L* (4 4) and 10*L* (5 5) (Evans & McKnight, 1959), the symbols in parentheses denoting

the number of consecutive layers stacked in cyclic or anticyclic order (Zhdanov, 1945). The layer sequence is automatically determined by the periodicity in the other three known ZnS structures: hexagonal $2L$ (1 1), cubic $3L$ $(3)_\infty$ and four-layer $4L$ (2 2) (Frondel & Palache, 1950).

One of the difficulties of structure determinations in ZnS has been the fact that in vapour-phase grown samples the regions which are crystallographically uniform have inconveniently small dimensions. In fact, X-ray work often yielded a mixture of several structures as well as one-dimensional stacking disorder (Strock & Brophy, 1955).

The layer sequence of a polytype can be determined, in principle, by comparison of the observed X-ray diffraction intensity distribution with the intensity distributions of all geometrically possible layer sequences. However, the number of possible layer sequences increases very rapidly with the period m of the polytype and therefore comparison with *all* possible sequences usually becomes impracticable even when a fast digital computer is used. Accordingly, for high polytypes special considerations have to be taken into account, in order to limit the number of layer sequences to be compared. In SiC, where a large number of polytypes are known, this is done by looking only for certain types of layer sequence (*e.g.* Krishna & Verma, 1962). There is no reason to believe that the same types of layer sequence are of special importance in ZnS as well; it will be seen that layer sequences of other types also occur.

For the present work ZnS crystals which contain uniform regions of convenient width were available. X-ray oscillation photographs were taken of the uniform regions. The observed intensity distributions were compared with intensities calculated by an electronic computer for possible layer sequences. The number of sequences to be calculated was reduced, in the case of higher polytypes, by using a recently found correlation between birefringence and structure (Brafman & Steinberger, 1966).

Experimental

The crystals used were grown by sublimation. Details of growing conditions as well as a table of typical cationic impurities can be found in a previous publication (Brafman, Alexander, Fraenkel, Kalman & Steinberger, 1964).

The crystals used were platelets, 30 to 200μ thick, the main faces being either (10.0) or (12.0) planes. Under the polarizing microscope they appeared to consist of parallel coloured strips. The strips are joined to each other along (00.1) planes. The colour changes are due to variations of the birefringence; this, in turn, is determined by the crystal structure. For the present work crystals were selected with wide regions (>0·1 mm) of uniform birefringence; X-ray analysis showed that the regions were uniform structurally as well. The optical band gaps and the birefringence of the crystals used have been reported previously (Brafman & Steinberger, 1966).

X-ray oscillation photographs were taken from the uniform regions with a 60 mm diameter camera mounted on a Hilger microfocus instrument. The crystals were oscillated around the c axis, which is common to all regions. The diameter of the X-ray beam emerging from the collimator was 0·1 mm. A polarizing microscope, mounted on the X-ray camera, served for adjusting the region to be investigated in the X-ray beam.

The reflexion spot intensities along (10.l) were estimated by visual comparison of the spots. This procedure gave very well reproducible estimates for nearby spots; it is, of course, somewhat less satisfactory for distant ones.

The degree of birefringence $\Delta n = n_e - n_0$, where n_e and n_0 are the extreme values of the refractive index, was determined by using a suitable compensator coupled with thickness measurements.

Computational methods

In case of the lower polytypes the unit translation in the c direction could be determined directly from distance measurements along (10.l) columns. This procedure immediately yields the period m of the polytype. For higher polytypes only a first estimate of m can be obtained in this way, because of the experimental error of the distance measurements. In such polytypes use was made of the periodicity of (10.l) structure factors with period m. Corresponding spots could therefore be easily identified by looking for groups of a few spots with similar intensity distributions. Counting the number of spots between two corresponding spots yields m unambiguously (Krishna & Verma, 1963).

From a knowledge of m, the possible reflexion intensity distributions were calculated with the IBM 7040 computer. This was done in two steps: (*a*) enumeration of the possible layer sequences for the given m; (*b*) calculation of the reflexion intensities.

(*a*) The layer sequences of an m-layer polytype are of the form $(a_1b_1\ a_2b_2 \ldots a_kb_k)$, where the a's and b's are natural numbers denoting the number of consecutive (00.1) planes, stacked in cyclic or anticyclic order respectively (Zhdanov, 1945).

Writing $\sum_{i=1}^{k} a_i = a$ and $\sum_{i=1}^{k} b_i = b$ one has

$$a+b=m \tag{1}$$

$$a-b=0 \pmod 3 . \tag{2}$$

Condition (2) ensures that the first and the last layers of the sequence shall not be in the same positions.

Conditions (1) and (2) yield all possible layer sequences, with many repetitions. A large part of the repetitions was avoided by imposing two further restrictions, namely

$$a \geq b \tag{3}$$

$$a_1 \geq a_j \quad j=2, \quad \ldots k . \tag{4}$$

The number of possible polytypes increases very steeply with m and full enumeration becomes impracticable even for the computer. Therefore for the higher polytypes ($26L$ and $28L$) use was made of the proportionality between the degree of birefringence Δn and the percentage of hexagonality α (Brafman & Steinberger, 1966). The number of elements, $2k$, of the Zhdanov symbol $(a_1 b_1 a_2 b_2 \ldots a_k b_k)$ can be calculated from α and m by the relation

$$2k = \alpha m/100 . \tag{5}$$

Thus the birefringence measurements restricted the possible sequences to those with a given number of elements, $2k$; only these layer sequences were enumerated by the computer.

(*b*) The calculation of the intensities was performed under the assumption that the structure of the Zn–S double layers is the same as in the hexagonal $2L$ (wurtzite) structure ($a = 3{\cdot}82$ Å), and that the distance between adjacent Zn layers is also the same as in wurtzite (3·13 Å). In the following, c is calculated from

$$c = m \times 3{\cdot}13 \text{ Å} .$$

For the calculation of the intensities I_{hkl}, only the structure factors and the Lorentz correction were taken into account:

$$I_{hkl} \propto (f_{Zn}^2 + f_S^2 + 2 f_{Zn} f_S \cos 2\pi lp)(A_{Zn}^2 + B_{Zn}^2) \times (1 + \cos^2 2\theta)/\sin 2\theta . \tag{6}$$

Here f_{Zn} and f_S are the zinc and sulphur atomic structure factors. $p = 3/(4m)$*, θ is the Bragg angle. A_{Zn} and B_{Zn} are given by

$$A_{Zn} = \Sigma \cos 2\pi(hx + ky + lz) \tag{7a}$$

$$B_{Zn} = \Sigma \sin 2\pi(hx + ky + lz) \tag{7b}$$

where the summations are over the Zn atoms in the unit cell and xyz denote the coordinates of these atoms.

* In all ZnS polytypes the coordinates of the S atoms are those of the Zn atoms + (00p).

Results

10L *polytype*

The (10.l) column of the X-ray oscillation photograph around the c axis is reproduced in Fig. 1. Note in this and in the following photographs the absence of 'smearing out' between the spots; it follows that no one-dimensional stacking disorder was evident in the uniform regions investigated. Sixteen 10L polytypes, differing in layer sequence, may exist; all corresponding intensities were calculated. Table 1 shows the comparison of (10.l) observed intensities with that of the sequence (8 2). It is seen that the fit is very good. None of the other sequences gave even an approximate fit. The Zhdanov symbol of the observed polytype is thus (8 2) and the ABC sequence (Ramsdell, 1947) is

$$ABCABCABAC$$

On hexagonal axes

$$a = 3{\cdot}82 , \quad c = 31{\cdot}3 \text{ Å}.$$

The hexagonal unit cell has

10Zn at 0,0,0 r,s,z $s,r,2z$ 0,0,3z $r,s,4z$ $s,r,5z$ 0,0,6z $r,s,7z$ 0,0,8z $s,r,9z$

where $z = \frac{1}{10}$, $r = \frac{2}{3}$, $s = \frac{1}{3}$.

Percentage of hexagonality: $\alpha = 20$. Birefringence at 5460 Å: $\Delta n = 4{\cdot}8 \times 10^{-3}$ (Brafman & Steinberger, 1966).

14L *polytype*

The (10.l) column is reproduced in Fig. 2. Table 2 shows the comparison of (10.l) observed intensities with that of the only fitting sequence (5 4 2 3). Thus the ABC sequence is

$$ABCABACBABCBAC .$$

On hexagonal axes

$$a = 3{\cdot}82 , \quad c = 43{\cdot}82 \text{ Å} .$$

The hexagonal unit cell has

14Zn at 0,0,0 r,s,z $s,r,2z$ 0,0,3z $r,s,4z$ 0,0,5z $s,r,6z$ $r,s,7z$

Table 1. *Comparison of calculated and observed* (10.l) *intensities for the* 10L (8 2) *polytype*

l	Calc.	Obs.	l	Calc.	Obs.	Further observed relations between intensities
0	5912	*s*				
1	9556	*vs*	$\bar{1}$	1598	*vw*	$\bar{3} > \bar{4}$
2	11677	*vs*	$\bar{2}$	914	*vw*	$7,6 > 1,2,3$
3	12018	*vs*	$\bar{3}$	153540	*vvs*	$7,6 < 4,5,\bar{5}$
4	11225	*vs*	$\bar{4}$	67115	*vvs*	$\bar{1} > \bar{2}$
5	10828	*vs*	$\bar{5}$	10828	*vs*	
6	20748	*vs*	$\bar{6}$	3470	*s*	
7	25882	*vs*	$\bar{7}$	2012	*vw*	
8	161	*a*	$\bar{8}$	2055	*w*	
9	355	*vw*	$\bar{9}$	2121	*w*	

$0,0,8z \quad r,s,9z \quad s,r,10z \quad r,s,11z$
$0,0,12z \quad s,r,13z$

where $z=\frac{1}{14}$, $r=\frac{2}{3}$, $s=\frac{1}{3}$.
Percentage of hexagonality: $\alpha=28{\cdot}6$.
Birefringence: $\Delta n=7{\cdot}1\times10^{-3}$ (Brafman & Steinberger, 1966).

Table 2. *Comparison of calculated and observed* (10.*l*) *intensities for the* 14*L* (5 4 2 3) *polytype*

l	Calc.	Obs.	*l*	Calc.	Obs.
0	4112	*w*			
1	1630	*vw*	$\bar{1}$	13267	*vs*
2	9903	*vs*	$\bar{2}$	8056	*s*
3	19379	*vs*	$\bar{3}$	29630	*vs*
4	100916	*vs*	$\bar{4}$	42963	*vs*
5	3592	*vw*	$\bar{5}$	91644	*vs*
6	70202	*vs*	$\bar{6}$	14367	*vs*
7	22332	*vs*	$\bar{7}$	22978	*vs*
8	6845	*w*	$\bar{8}$	33444	*vs*
9	25081	*vs*	$\bar{9}$	983	*a*
10	9746	*s*	$\bar{10}$	22877	*vs*
11	7642	*w*	$\bar{11}$	4968	*vw*
12	2685	*a*	$\bar{12}$	3300	*vw*

24L polytype

The (10.*l*) column is represented in Fig. 3. The distances between the spots are those corresponding to an 8-layer polytype but they are situated asymmetrically with respect to the zero layer; the zero layer divides the distance between spots neighbouring to it in the ratio 1:2. The structure is thus of rhombohedral symmetry. For the layer sequence determination it was thus sufficient to take into account the rhombohedral 24*L* polytypes only.

Table 3 shows the comparison of (10.*l*) observed intensities with the only fitting sequence $(5\ 3)_3$*. The *ABC* sequence is

ABCABACBCABCACBABCABCBAC

On hexagonal axes $a=3{\cdot}82$, $c=75{\cdot}12$ Å.
The hexagonal unit cell has

8Zn at $0,0,0 \quad 0,0,3z \quad 0,0,5z \quad 0,0,9z$
$0,0,12z \quad 0,0,15z \quad 0,0,18z \quad 0,0,22z$
8Zn at $\frac{1}{3},\frac{2}{3},\frac{1}{3}$ plus the above coordinates
8Zn at $\frac{2}{3},\frac{1}{3},\frac{2}{3}$ plus the above coordinates

where $z=\frac{1}{24}$.
Percentage of hexagonality: $\alpha=25$.
Birefringence: $6{\cdot}1\times10^{-3}$ (Brafman & Steinberger, 1966).

26L polytype

The (10.*l*) column is represented in Fig. 4. The number of possible 26*L*-layer sequences being too large, the number of those to be calculated was restricted by considering only Zhdanov sequences compatible with α-values obtained from the observed birefringence. Measurement yielded that $\Delta n=3{\cdot}6\times10^{-3}$. This is near to $\Delta n=3{\cdot}7\times10^{-3}$ calculated from $\alpha=15{\cdot}4$ ($k=2$). Clearly other values of k can be disregarded, as $k=1$ would yield $\Delta n=1{\cdot}85\times10^{-3}$ and $k=3$ $\Delta n=5{\cdot}54\times10^{-3}$. Thus for the comparison only Zhdanov sequences with 4 elements had to be considered. Table 4 shows the comparison of (10.*l*) observed intensities with those of the only fitting sequence (17 4 2 3). The *ABC* sequence is

ABCABCABCABCABCABACBABCBAC.

On hexagonal axes

$a=3{\cdot}82$, $c=81{\cdot}38$ Å.

The hexagonal unit cell has

26Zn at $0,0,0 \quad r,s,z \quad s,r,2z \quad 0,0,3z \quad r,s,4z$
$s,r,5z \quad 0,0,6z \quad r,s,7z \quad s,r,8z \quad 0,0,9z$
$r,s,10z \quad s,r,11z \quad 0,0,12z \quad r,s,13z$
$s,r,14z \quad 0,0,15z \quad r,s,16z \quad 0,0,17z$
$s,r,18z \quad r,s,19z \quad 0,0,20z \quad r,s,21z$
$s,r,22z \quad r,s,23z \quad 0,0,24z \quad s,r,25z$

where $z=\frac{1}{26}$, $r=\frac{2}{3}$, $s=\frac{1}{3}$.

Table 3. *Comparison of calculated and observed* (10.*l*) *intensities for the* 24*L* $(5\ 3)_3$ *polytype*

l	Calc.	Obs.	*l*	Calc.	Obs.
2	27641	*w*	$\bar{1}$	7207	*vw*
5	127953	*vs*	$\bar{4}$	93246	*s*
8	507616	*vvs*	$\bar{7}$	175818	*vs*
11	139621	*vs*	$\bar{10}$	162029	*vs*
14	69675	*s*	$\bar{13}$	90019	*s*
17	40452	*w*	$\bar{16}$	126572	*vs*
20	28581	*w*	$\bar{19}$	33938	*w*
23	3543	*a*	$\bar{22}$	11633	*w*

28L polytype

The (10.*l*) column is represented in Fig. 5. The number of 28-layer sequences to be compared was restricted as in the case of 26*L*. For $k=1$ $\Delta n=1{\cdot}71\times10^{-3}$; for $k=2$ $\Delta n=3{\cdot}43\times10^{-3}$; for $k=3$ $\Delta n=5{\cdot}14\times10^{-3}$. The measured value of Δn was 3·6. Thus $k=2$; only Zhdanov sequences with four elements had to be considered. Table 5 shows the comparison of (10.*l*) observed intensities with those of the only fitting sequence (9 5 5 9). The *ABC* sequence is

ABCABCABCBACBABCABCBACBACBAC.

On hexagonal axes

$a=3{\cdot}82$, $c=87{\cdot}64$ Å.

The hexagonal unit cell has

* This is the only polytype structure reported in the present work which has an SiC counterpart (Gomes de Mesquita, 1965).

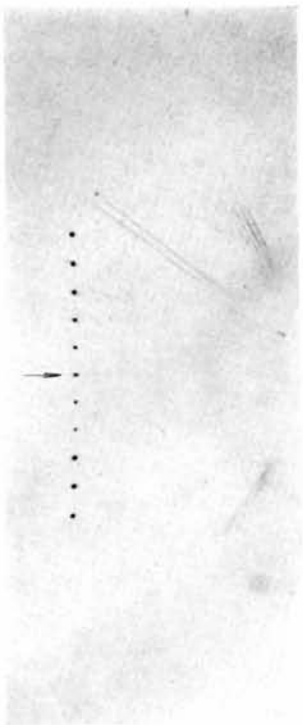

Fig. 1. (10.*l*) column of an oscillation photograph around the *c* axis of the 10*L* polytype. Cu $K\alpha$ radiation, 60 mm diameter camera ($\times 3$). The position of the zero layer is indicated by an arrow.

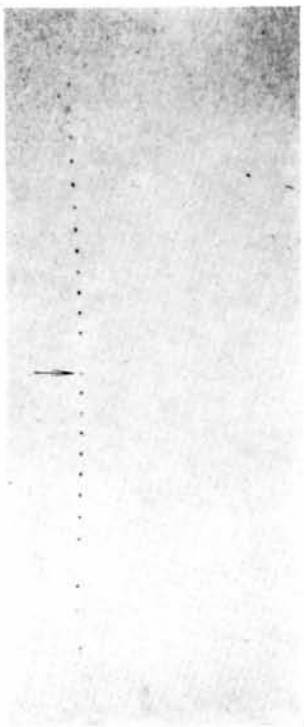

Fig. 2. As Fig. 1, but for 14*L* polytype.

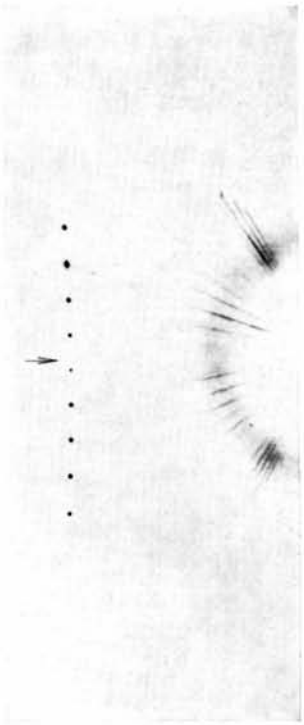

Fig. 3. As Fig. 1, but for 24*L* (rhombohedral) polytype.

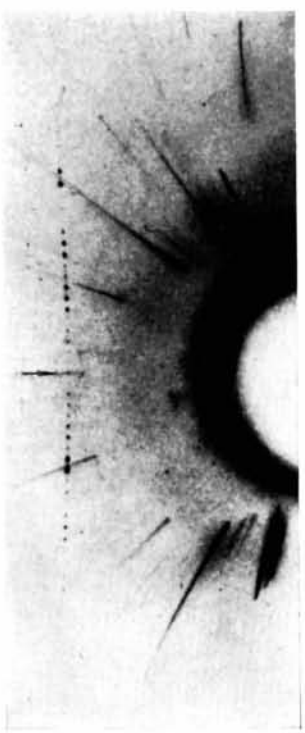

Fig. 4. As Fig. 1, but for 26*L* polytype.

Fig. 5. As Fig. 1, but for 28*L* polytype.

[*To face p.* 350

28Zn at 0,0,0 r,s,z $s,r,2z$ 0,0,3z $r,s,4z$
$s,r,5z$ 0,0,6z $r,s,7z$ $s,r,8z$ $r,s,9z$
0,0,10z $s,r,11z$ $r,s,12z$ 0,0,13z
$r,s,14z$ $s,r,15z$ 0,0,16z $r,s,17z$
$s,r,18z$ $r,s,19z$ 0,0,20z $s,r,21z$
$r,s,22z$ 0,0,23z $s,r,24z$ $r,s,25z$
0,0,26z $s,r,27z$

where $z=\frac{1}{28}$, $r=\frac{2}{3}$, $s=\frac{1}{3}$.

Space does not permit publication of the intensity distributions of the several hundred layer sequences of the various polytypes calculated by the computer. It should, however, be emphasized that except for the layer sequences given above there were no other layer sequences in any case which gave even a rough fit with the observed intensities.

Discussion

The present work demonstrates that the use of birefringence results makes it possible to shorten the calculations leading to identification of ZnS polytype layer structures. The linear relation used between the degree of birefringence and percentage of hexagonality had been obtained from data on simple structures (Brafman & Steinberger, 1966); the validity of this relation is further substantiated by the excellent fit of the intensities in the case of 26L and 28L polytypes. The calculations leading to the identification of layer sequences are, however, too lengthy in the case of the higher polytypes even if the birefringence results are taken into account. In fact, the structures of 40L and 120L polytypes previously mentioned (Brafman &

Table 4. *Comparison of calculated and observed* (10.l) *intensities for the* 26 L (17 4 2 3) *polytype*

l	Calc.	Obs.	l	Calc.	Obs.	Further observed relations between intensities
0	3932	*vw*				
1	2718	*a*	$\bar{1}$	5168	*vw*	
2	2101	*a*	$\bar{2}$	13843	*w*	$\bar{9}>\bar{8}$
3	9926	*w*	$\bar{3}$	13138	*w*	$7>8$
4	6568	*vw*	$\bar{4}$	7661	*vw*	$11\simeq 12<8$
5	1670	*a*	$\bar{5}$	21841	*s*	$\bar{5}\simeq\bar{6}<6$
6	42268	*s*	$\bar{6}$	24890	*s*	$\bar{14}>\bar{13}\simeq\bar{5}$
7	94833	*vs*	$\bar{7}$	9274	*vw*	$\bar{2}\simeq\bar{3}>3$
8	73463	*vs*	$\bar{8}$	295861	*vvs*	
9	11717	*w*	$\bar{9}$	640129	*vvs*	
10	14231	*w*	$\overline{10}$	8678	*vw*	
11	62950	*vs*	$\overline{11}$	16036	*w*	
12	64292	*vs*	$\overline{12}$	3304	*a*	
13	22151	*w*	$\overline{13}$	22150	*s*	
14	2203	*a*	$\overline{14}$	42862	*s*	
15	7318	*vw*	$\overline{15}$	28727	*s*	
16	2872	*a*	$\overline{16}$	4710	*a*	
17	168364	*vs*	$\overline{17}$	3081	*a*	
18	69243	*s*	$\overline{18}$	17193	*vw*	
19	2151	*a*	$\overline{19}$	21995	*w*	

Table 5. *Comparison of calculated and observed* (10.l) *intensities for the* 28L (9 5 5 9) *polytype*

l	Calc.	Obs.*	l	Calc.	Obs.	Further observed relations between intensities
0	3918	*vw*	14	22083	*s*	$9>11>8$
1	8533	*w*	15	3324	*vw*	$5\simeq 7>6$
2	5554	*w*	16	4430	*vw*	$18<17,19,20$
3	1612	*vw*	17	74717	*s*	$23>21<22$
4	3467	*vw*	18	21124	*s*	$1>2$
5	29266	*s*	19	72770	*s*	$0>4>3$
6	11002	*s*	20	35467	*s*	
7	25932	*s*	21	6189	*vw*	
8	153927	*vvs*	22	2870	*vw*	
9	301819	*vvs*	23	8602	*vw*	
10	75950	*vs*	24	1163	*a*	
11	211922	*vvs*	25	620	*a*	
12	9215	*w*	26	2447	*vw*	
13	4844	*vw*	27	4290	*vw*	

* The observed intensities were symmetrical with respect to the zero line ($l=0$).

Steinberger, 1966) have for this reason not yet been determined.

Comparison of published ZnS polytype layer sequences with those known in SiC immediately demonstrates the fact that the numbers of elements in the Zhdanov symbols of ZnS polytypes are, in general, smaller than those reported in SiC polytypes. In other words, the percentage of hexagonality of ZnS polytypes tends to be lower.

For SiC polytypes, the theory which explains the growth of most observed polytypes is that of Frank (1961) and Mitchell (1957), as modified by Krishna & Verma (1965). This theory is based on the fact that in SiC a thin platelet with (00.1) faces is at first formed. The platelet may have one of the structures 4*L*, 6*L* or 15*L* (these being the most frequent SiC structures). As a result of buckling, a step appears. Its height is usually less than the *c* dimension of the unit cell of the basic structure. A screw dislocation is thus formed which ensures further growth; the Burgers vector of this dislocation is a non-integral multiple of the basic *c* translation.

It is very unlikely that for polytypism in ZnS the above model is correct in its present form. First, in the initial stages of the growth thin *needles* form with the axis [00·1]; such needles cannot buckle in the way proposed for platelets. Secondly, among the observed ZnS polytypes there are some which have large elements in their Zhdanov sequence [*e.g.* (17 4 2 3)], whereas on the basis of the Mitchell–Verma model such large elements can not be expected.

A modification of the above model, or else a quite different one is, therefore, needed for the explanation of polytypism in ZnS. It seems to be, however, premature to contemplate such a model, since the number of known ZnS polytypes is still too low for meaningful comparison of experiment with theory.

References

BRAFMAN, O., ALEXANDER, E., FRAENKEL, B. S., KALMAN, Z. H. & STEINBERGER, I. T. (1964). *J. Appl. Phys.* **35**, 1855.

BRAFMAN, O. & STEINBERGER, I. T. (1966). *Phys. Rev.* **143**, 501.

EVANS, H. T. & MCKNIGHT, E. T. (1959). *Amer. Min.* **44**, 1210.

FRANK, F. C. (1951). *Phil. Mag.* **42**, 1014.

FRONDEL, C. & PALACHE, C. (1950). *Amer. Min.* **35**, 29.

GOMES DE MESQUITA, A. H. (1965). *Acta Cryst.* **18**, 128.

KRISHNA, P. & VERMA, A. R. (1962). *Z. Kristallogr.* **117**, 1.

KRISHNA, P. & VERMA, A. R. (1963). *Proc. Roy. Soc.* A, **272**, 490.

KRISHNA, P. & VERMA, A. R. (1965). *Z. Kristallogr.* **121**, 36.

MITCHELL, R. S. (1957). *Z. Kristallogr.* 109, 1.

RAMSDELL, L. S. (1947). *Amer. Min.* **32**, 64.

STROCK, L. W. & BROPHY, V. A. (1955). *Amer. Min.* **40**, 94.

ZHDANOV, G. S. (1945). *C. R. Acad. Sci. URSS*, **48**, 43.

Acta Cryst. (1967). **22**, 352

The Crystal Structure of Adamantane: An Example of a False Minimum in Least Squares

BY JERRY DONOHUE* AND STEWARD H. GOODMAN

Department of Chemistry, University of Southern California, Los Angeles, California, U.S.A.

(*Received* 18 *April* 1966 *and in revised form* 6 *July* 1966)

A least-squares refinement of the structure of the low temperature form of adamantane, starting with molecules having symmetry $\bar{4}3m$, and tilted 9° about the *c* axis, refines to a structure not significantly different, and a reduction of the residual from 3·92 to 3·11. On the other hand, if the refinement is started at the published structure, the parameters of which correspond to rather distorted molecules, a structure not significantly different from *this* starting point results, and a reduction of the residual from 15·49 to 14·34.

Introduction

A recent study of the crystal structure of the low temperature phase of adamantane (Nordman & Schmitkons, 1965, hereinafter referred to as NS) in which it was reported that the molecule departed significantly from $\bar{4}3m$ symmetry by being compressed along one of its $\bar{4}$ axes, prompted us to examine this structure further, partly because NS stated that 'there is no readily apparent interpretation of this effect in terms of close intermolecular contacts', and partly because of current interest in these laboratories in this phase and its relation to the high temperature phase (Dows & Rubenstein, 1965). The low temperature phase, according to NS, is tetragonal, space group $P\bar{4}2_1c$, $a=6{\cdot}60$, $c=8{\cdot}81$ Å, $Z=2$. Precession data (Cu $K\alpha$, 53 visually estimated F_{obs}) were refined by least squares, optimizing seven positional parameters for the carbon atoms, twelve positional parameters for the hydrogen

* Present address: Department of Chemistry, University of Pennsylvania, Philadelphia, Pennsylvania, U.S.A.